International Journal of Engineering Trends and Technology
ISSN: 2231–5381 / https://doi.org/10.14445/22315381/IJETT-V71I11P207

Volume 71 Issue 11, 69-83, November 2023

Review Article

A Review of the Bamboo-Based Activated Carbon: Wastewater Treatment & Supercapacitor Device Applications

Ho Soonmin[1], Noor Afeefah Nordin[2], R. Rajesh Kannan[3]

[1]*Faculty of Health and Life Sciences, INTI International University, Putra Nilai, Negeri Sembilan, Malaysia.*
[2]*Institute of Power Engineering, National Energy University, Jalan IKRAM-UNITEN, Kajang, Selangor, Malaysia.*
[3]*Department of Chemical Engineering, Annamalai University, Annamalai Nagar, Tamilnadu, India.*

[1]*Corresponding Author : soonmin.ho@newinti.edu.my*

Received: 23 June 2023 Revised: 03 August 2023 Accepted: 20 September 2023 Published: 04 November 2023

Abstract *- Carbonaceous source materials have been employed to prepare activated carbon via the carbonization process and activation technique. During the synthesis of the activated carbon, some activating agents (basic, neutral, and acidic forms) have been used to enlarge the surface area, open the pores, and increase the adsorption power. In this work, the obtained bamboo-based activated carbon showed a large surface area, high porosity structure, and desired surface functionalization. Therefore, it is considered a great adsorbent for air purification and wastewater treatment. Adsorption data were fully supported by the Langmuir model or Freundlich isotherm. Apart from pollutants and heavy metal adsorption, activated carbon has been broadly utilized in the electrochemical industry to fabricate supercapacitor electrodes. Unique properties (porous microstructure and high adsorption capacity make it appropriate for the adsorption and desorption of electrolyte ions in non-Faradaic processes without involving chemical reactions. Experimental results confirmed that the prepared carbons showed high-rate capability, excellent capacitance value and long cycle life.*

Keywords *- Activated carbon, Wastewater treatment, Supercapacitor devices, Absorption, Langmuir model.*

1. Introduction

Activated Carbon (AC) is technically referred to as carbonized materials that are highly porous and have a larger surface area [1]. To date, the demand for activated carbon has gradually increased [2], and the market value was 1,666 kilotons (in 2020). It is expected that the Compound Annual Growth Rate for activated carbon (2021–2026) will be more than 3% due to the current demand, especially in industrial and municipal wastewater treatment. The market for activated carbon is anticipated to grow significantly through 2028 due to the demand from various sectors, including wastewater [3], air purification [4], automotive, metal recovery [5], food and beverage processing, and pharmaceutical drug manufacturing process [6]. Commercial activated carbons are generally produced from non-renewable precursors such as coal, petroleum coke, and lignite [7]. However, these precursors incurred high processing costs for the manufacturers.

Further, alternative materials have been explored (agricultural waste/biomass) aimed at some cost reduction [8]. Currently, there are three types of activated carbon, namely pellets, granular and powder [9]. Granular and powdery were generally the most widely used due to their distinct properties [10]. In terms of composition, up to 90% of activated carbon consists of carbon, making it a very varied adsorbent substance with an excellent standard of permeability and expansive expanse area [11]. The distinct adsorption characteristics rely on the activated carbon's current functional groups, which are primarily obtained from precursors, activation steps, and heat purifying [12].

Bamboo is a fast-growing lignocellulosic material available throughout the year [13-15]. It was reported in the literature that bamboo contains moderate-high carbon (48.64 %) and a relatively low percentage of hydrogen (6.75 %), nitrogen (0.14 %), and sulphur (0.11 %). Apart from that, bamboo is also well known for its low density, high mechanical strength and high stiffness [16]. Considering its carbon content, bamboo has become one of the chosen materials [17] for activated carbon production using several methods.

Supercapacitor is emerging as one of the advanced energy storage materials available in the market and is used for various purposes ranging from domestic uses to high-end

applications. Supercapacitors were developed to bridge the gap between conventional capacitors and lithium-ion batteries (LIBs) in the context of energy storage and power bursts [18]. The performance of a supercapacitor can be evaluated by measuring its electrochemical properties, which differ according to the materials chosen for its electrode and electrolyte. The supercapacitors were reported to have low discharge time (1-10s) and enhanced cyclic stability (>30 000h) compared to LIB (60-100min) and (>500 h), respectively [19].

In this work, bamboo was chosen as the precursor to produce activated carbon through a series of carbonization and activation processes. Physical properties, porosity structures and textural behaviors have been studied using different tools. Removal of dye, pollutant gases, heavy metals, antibiotics, and organic compounds has been reported. Adsorption data will be studied using various isotherms (Freundlich model, Langmuir isotherm, Temkin model). Finally, the performance of supercapacitor devices will be discussed.

2. Literature Survey

2.1. Activated Carbon

It was noted that agricultural refuse [20], animal by-products, and commercial by-products could serve as starting materials for the synthesis of activated carbon. Agro-industrial residues are among the most popular because of their renewability, high mechanical strength, affordability, availability, and low ash contents [21]. The structure of the basic materials and the manufacturing procedures could affect the maximal adsorptive capacity of activated carbon.

There are four major processes of activated carbon, namely pyrolysis, carbonization, physical activation, and chemical activation. Several activating agents (potassium hydroxide (KOH), zinc chloride ($ZnCl_2$), sulfuric acid (H_2SO_4), sodium hydroxide (NaOH) and phosphoric acid (H_3PO_4)) have been used in the chemical activation process [22]. These activating agents (basic, acidic, and neutral forms) could degrade cellulosic materials [23] and develop the pore structure. On the other hand, several properties of products (specific surface area and pore size distribution) strongly depend on the degree of impregnation [24]. It was noted that the presence of some impurities (phosphorus and zinc) could be seen in the obtained products.

The thermochemical process (pyrolysis process) converts organic material into vapor or liquid fuels when the temperature is very high without halogens. Pyrolysis is a synchronous [25], irreversible process that modifies both an object's physical condition and chemical composition [26]. Normally, increasing the reaction heat caused char content and the percentage of yield to decrease, while increasing the pyrolysis temperature resulted in the output of gases and liquid components to rise and the yield of solids to decrease [27]. On the other hand, raising the temperature results in a decline in volatile matter while raising the yield percentage [28]. As a result, good quality of the activated carbon could be synthesized at higher temperatures.

Additionally, raising the temperature may cause a reduction in char output because of the significant breakdown of char residues or because of the secondary breakdown of biomass at elevated temperatures [29]. In the physical activation process, pyrolysis happened, followed by gasification (carbon dioxide, steam, and oxygen) of the charcoal obtained. The physical activation process could produce a low yield and a lot of pyrolytic oil. A higher yield percentage with little pyrolytic oil could be observed during the chemical activation process. The starring material was treated with chemical activation agents, followed by heating (450 °C to 700 °C) in the kiln. Carbonization requires heat (300 °C to 900 °C) in the absence of air. It converts organic matter into coal (drives off the volatile components).

The absorption or adsorption process is typically what is meant when the term "sorption" is used [30]. During the adsorption process, absorbate will be absorbed into the absorbent. As highlighted in the separation process, a portion of the fluid-phase constituents were moved to the adsorbent surface. The propensity of molecules in the liquid stage to attach to the solid surface can be used to demonstrate surface adsorption. Adsorption, on the other hand, only affects the absorbent surface and visitor molecules, whereas the absorption process describes the aptitude of some substances to take contaminants from the solution and incorporate them into their structure [31, 32].

Physical adsorption happened when the adsorbate molecules were held by Van der Waals forces [33]. The heat was very weak and reversible. The physical adsorption was non-specific and always multilayers. Chemical adsorption happened [34] when the adsorbate molecules were held on the surface of the adsorbent via chemical forces (covalent chemical bonding). The heat was high if compared to physical adsorption. It is highly specific and always monolayer [35].

2.2. Bamboo-Based Activated Carbon Adsorbent

Ruthenium complex dye was used in dye-sensitized solar cells (as photosensitizers). This dye showed excellent stability (in an oxidized state) and unique photo-electrochemical behaviors. The maximum adsorption capacity [36] of cis-bis(isothiocyanato) bis(2,2’-bipyridyl-4,4’-dicarboxylato ruthenium (II) reached 1.5 mg/g (NaOH activation, carbonization process). Masanizan and co-workers [37] studied the removal of dye wastes using potassium hydroxide-activated and copper-modified activated carbon. Adsorption studies (correlation of Freundlich model=0.927, correlation of pseudo-second order model=0.996, maximum adsorption capacity (Langmuir model) =64.4 mg/g) have been described. Thermodynamic studies confirmed that the adsorption process was a spontaneous reaction and feasible.

Ciprofloxacin was used to treat skin infections, diarrhea, typhoid fever, and respiratory tract infections. It was considered an antibiotic and could be taken in several ways (ear, mouth, or eye drops). Surface area (2237 m^2/g), total pore volume (1.23 cm^3/g) and micropore ratio (greater than 90%) have been investigated in the optimized conditions (impregnation ratio=3:1, activation agent=phosphoric acid & K_2CO_3, activation temperature=750°C). Adsorption data supported the Langmuir isotherm and pseudo-second-order kinetic model [38]. The highest removal of ciprofloxacin from water reached 613 mg/g. Peng and co-workers [39] reported that the adsorption process happened in weakly acidic conditions (spontaneous reaction and endothermic), and the adsorption amount increased when the zwitterionic form was increased. In addition, these amine-functionalized magnetic carbons indicated good recyclability after five recycles (keep more than 80% removal). Xiaoming and co-workers [40] described that adsorption capacity could be improved by adding alkaline nitrogen functionalities. Research findings confirmed that maximum adsorption was found at the lowest solubility due to hydrophobic interaction. A better correlation was observed in the pseudo-second-order isotherm and Langmuir model. According to thermodynamic studies, the adsorption capacity increases when the temperature increases.

Lead (Pb) was a cumulative toxicant which was very harmful to young children. The major world lead consumption was lead acid batteries, followed by paint, pigment, toys, jewelry, and stained glass. Lead also causes long-term harm in adults (kidney damage and high blood pressure). Carbonization (muffle furnace, 180 minutes and 500 °C) and activation process (zinc chloride) have been used to synthesis bamboo stick-based activated carbon. Ash (6.7%, pH (pH=6.6), moisture (2.95%), porosity (0.89), surface area (359 m^2/g), bulk density (0.56 g/cm^3), specific gravity (1.28), and carbon yield (27.69%) were reported. Removal efficiency of lead achieved 96.09%, at pH 11, within 60 minutes using 50 μm (adsorbent). The adsorption process obeyed Freundlich isotherm (K_f value was 2.128 mg/g), indicating that the chemisorption process and multilayer could be observed on the adsorbent surface [41].

Most rocks and soils consisted of cadmium. It was observed as a mineral combined with sulfur, chlorine, and oxygen. Generally, cadmium will be released into the environment via different ways (forest fire, volcanoes, wind, rain, and mining operations). Cadmium is a cancer-causing agent that causes kidney disease, irritates the stomach, and can damage the lungs. Removal efficiency of cadmium reached 83.44%, at pH 9, within 90 minutes using 50 μm (adsorbent). The adsorption process supported the Freundlich model (K_f value was 7.01 mg/g), confirmed that a multilayer layer could be seen, and the chemisorption process happened [41]. Synthesis of adsorbent through KOH activation (impregnation time=24 hours, impregnation ratio=3:1). The percentage of adsorption of Cd increased [42] when the pH was increased (up to pH 5.5). The highest adsorption capacity reached 87.4% at pH 5.5. Fa and co-workers concluded that the Langmuir model (R^2=0.9932, maximum adsorption capacity=12.08 mg/g) was perfectly matched if compared to the Temkin isotherm (R^2=0.990) and Freundlich model (R^2=0.9892). The adsorption rate is very fast removed; 40% of cadmium was removed within 5 minutes and finally reached equilibrium (after 6 hours). The adsorption capacity increases with increasing the pH and initial cadmium concentration.

Formaldehyde is a volatile organic compound that can pollute the outdoor and indoor air. Formaldehyde could be used in paper product coatings, insulation materials, plywood, glues, and adhesives. A low concentration of formaldehyde could be removed using adsorbent. Bamboo charcoal is activated with boric acid solution and then impregnated with ammonium acetate to develop the porosity structure. Specific surface area, microporous volume and total pore volume were 240.09 m^2/g, 0.12 cm^3/g and 0.27 cm^3/g, respectively [43]. Removal of formaldehyde reached 98.89% and obeyed pseudo-second-order kinetic (indicated physical chemical combined adsorption process). In addition, these carbons showed excellent recyclability after five recycles (keep 82.8% removal). Rengga and co-workers [44] reported that copper-attached activated carbon absorbed 29% higher than original activated carbon, while silver-attached carbon indicated 1.6 times higher at an equilibrium concentration of 8 ppm (formaldehyde). It was noticed that silver particles were more uniformly distributed on adsorbent with bigger size (5-40 nm) if compared to copper cluster (2-10 nm), according to SEM images and TEM analysis. Wara and co-workers [45] reported the properties of silver (Ag) attached to activated carbon using field emission scanning electron microscopy (less pore in the product), TEM technique (silver was well distributed on the carbon), Brunauer-Emmett-Teller technique (silver reduced surface area), and the energy dispersive X-ray analysis technique (the presence of silver in the product). According to the continuous fixed bed column experiments, the adsorbate mass removed by silver attached carbon is 2.36 times more than the original carbon. Thermodynamic studies have been conducted [46], free energy (-20.386 to -22.094 J/mol), enthalpy (-675.84 J/mol) and entropy (49.5 J/mol.K) were described. The experimental results fitted well with Langmuir isotherm with maximum adsorption capacities (91mg/g-110 mg/g). The highest adsorption capacity of silver-loaded bamboo-based carbon aerogel (5% Ag) was 42 mg/g (25 ppm formaldehyde concentration), 5.25 times that of bamboo-based carbon aerogel [47]. Chemical sorption happened between the hydroxyl group (adsorbent) and carbonyl (formaldehyde). Transmission electron microscopy (TEM) analysis (figure 1) confirmed that silver was evenly distributed in the space of spots, and the average size (silver particle) was 25.42 nm.

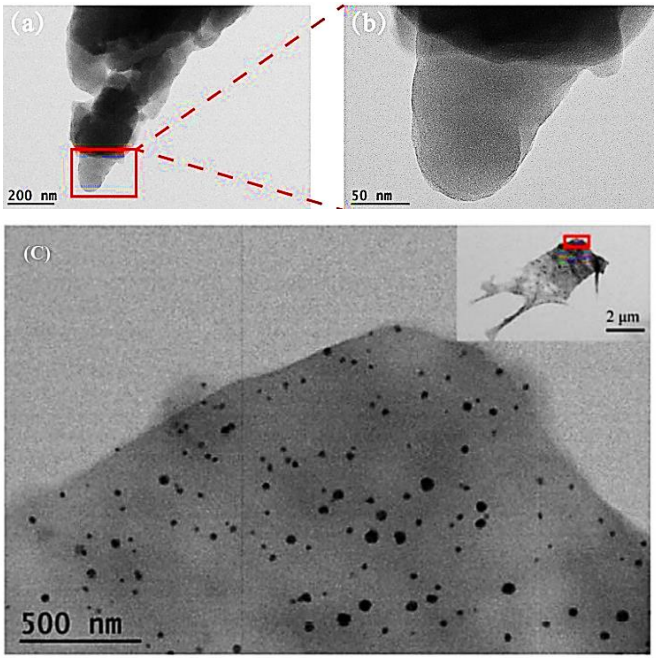

Fig. 1 TEM of (a,b) Bamboo-based carbon aerogel (c) 5% Ag/bamboo-based carbon aerogel [47]

Methylene blue was employed as a dye (thiazine dye) and medication (treat methemoglobinemia). It is carcinogenic, toxic, and non-biodegradable. Further, it threatens human health (harmful to lymphoids and liver) and environmental safety as well. Bambusa vulgaris-based activated carbon was produced [48] via the activation process (temperature=500 °C, residence time= 60 minutes, water steam flux=100 mL/min, nitrogen flux=80 mL/min, heating rate=10 °C/min). Experimental results showed that the adsorption process occurred rapidly at 1 hour (36.09 %), 3 hours (49.52%) and 6 hours (86.84 %), reached equilibrium after 12 hours (99.7%), and dye was fully adsorbed (99.86 %) within 24 hours. The adsorption process was favorable (dimensionless equilibrium=0.052), and the highest adsorption capacity was 374.75 mg/g. Modification of activated carbon was carried out using the microwave oven in a nitrogen atmosphere. Surface acidic groups were reduced, but pore size and pore volume increased during the modification process [49]. Kinetic studies revealed that Freundlich and pseudo-second-order models fitted well for all carbons. The carbon dioxide (CO_2) and potassium hydroxide (KOH) were applied [50] in the specific conditions (120 minutes and 850 °C). Removal of methylene blue reached 454.2 mg/g (Langmuir model) and followed the pseudo-second-order model. The influence of pyrolysis time (pyrolysis temperature=1050 °C, heating rate=10 °C/min) was studied [51]. The yield (21.66% to 13.8%) and microporous fraction (65.96 to 22.61 %) dropped, but surface area (1456 to 2348 m^2/g) mesoporous volume (0.32 to 1.78 cm^3/g) and total pore volume (0.94 to 2.3 cm^3/g) increased with the pyrolysis time (2.5 hours to 10 hours). As shown in the SEM images, smooth morphology could be observed at short pyrolysis time, while different sizes and geometrics were detected at longer times (10 hours). A higher correlation in the Langmuir model (maximum adsorption capacity=495 to 1667 mg/g) if compared to the Freundlich model, representing more homogeneous adsorption occurred. Another activation agent, such as potassium carbonate (K_2CO_3), was used to produce adsorbent [52] via microwave oven (gas=nitrogen, irradiation power=800 W, irradiation time=15 minutes). In Figure 2, morphologies of raw bamboo waste (smooth surface), activated carbon (irregular pores, mesoporous structure, flake-type), and after adsorption (more compact, less porous) have been investigated using SEM technique. Thermodynamic parameters were investigated, free energy (-5.08 kJ/mol to -9.98 kJ/mol), enthalpy (35.67 kJ/mol) and entropy (0.13 kJ/mol.K) were described.

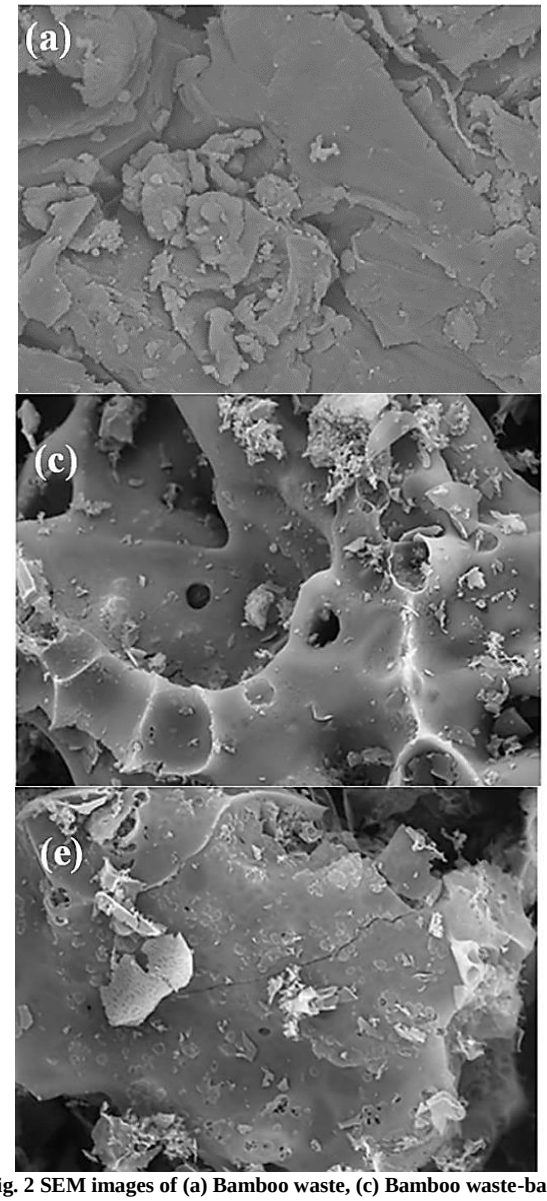

Fig. 2 SEM images of (a) Bamboo waste, (c) Bamboo waste-based activated carbon, and (e) Activated carbon after adsorption [52]

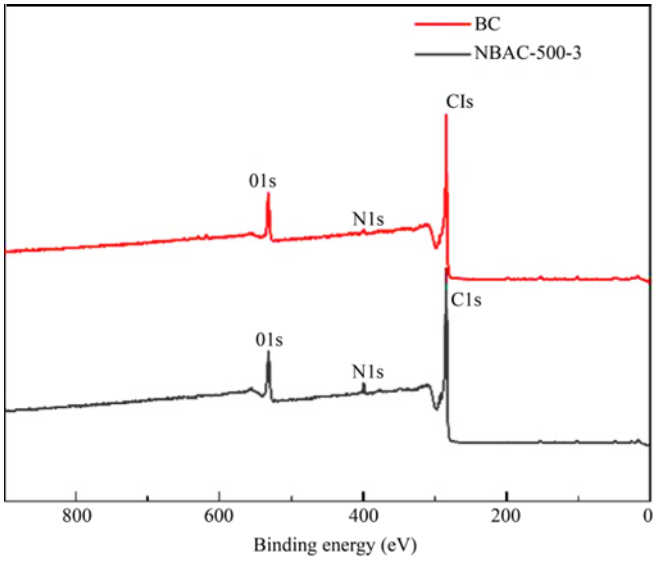

Fig. 3 XPS spectra of bamboo charcoal (BC) and nitrogen-doped activated carbon (NBAC) [55]

Norfloxacin is a quinolone antibiotic that can prevent bacteria growth. It was used to treat bacterial infections but not for viral infections. The adsorption process is endothermic and spontaneously happens in weakly acidic conditions, and the adsorption amount increases when the zwitterionic form is increased. Removal of norfloxacin obeyed the Langmuir model, and the saturated magnetization achieved 8.55 emu/g. In the desorption and regeneration investigations, these amines' functionalized magnetic carbons keep more than 80% (after 5 cycles).

Methanol is an organic chemical with the formula (CH_3OH). It was flammable, light, colorless and volatile. It is toxic because of metabolic products (cause metabolic acidosis and blindness). On the other hand, toluene is colorless, clear, and shows a distinctive smell. It could be used in glues, lacquers, and paints. Toluene causes systemic toxicity, skin irritation, and eye irritation. Nitrogen-doped activated carbon showed a larger specific surface area (2293.2 m^2/g) and microporosity structure (0.9 cm^3/g). Adsorption of methanol (capacity was 915.3 mg/g) is mainly controlled by electrostatic interaction between the methanol and carbon surface [53]. Removal of toluene (capacity=622.9 mg/g) is trapped via π-π dispersive interactions, and the aromatic ring was moved to the surface of the adsorbent. Monolithic activated carbon (produced from shrubby bamboo) showed excellent mechanical strength, higher carbon content and was very stable under wet conditions [54]. The highest adsorption capacity of toluene reached 350 mg/g in the optimized adsorbent (well-developed micropores).

Carbon dioxide gas is colourless and has a faint, sharp odor and sour taste. It was a greenhouse gas related to global warming. It could be used in urea, metal fabrication, food, and beverage production. Exposure to carbon dioxide causes tiredness, headaches, coma, asphyxia, dizziness, sweating, difficulty breathing and convulsions. High surface area (756-1489 m^2/g), narrowly distributed micropores and high nitrogen content could be seen in the nitrogen-doped activated carbon [55]. In x-ray photoelectron spectroscopy analysis (figure 3), three major peaks at 285 eV, 399 eV and 532 eV contributed to $C1_s$, $N1_s$ and $O1_s$, respectively, in all samples (bamboo charcoal and nitrogen-doped activated carbon). Experimental results revealed that a low dosage of sodamide could improve the adsorption performance. The maximum adsorption capacity (carbon dioxide) reached 4.95 mmol/g (at 1bar, 0 °C) in the highlighted conditions (sodamide/bamboo ratio=3:1, activation temperature=500 °C). The adsorption is a physical process, and the initial isosteric heat of adsorption is successfully achieved at 30-40 kJ/mol. Based on the adsorption/desorption experiment, these carbons keep 93 % after 10 cycles. The influence of charcoal powder size and the carbonized temperature was pointed out [56]. The maximum adsorption capacity could be observed when the powder size was 170 mesh if compared to other sizes (60 mesh and 100 mesh). It was noticed that the concentration of carbon dioxide reduced (from 1.854%, 1.169%, 1.099%, 1.012%, 0.946% to 0.836%) with increasing temperature (from 600, 700, 800, 900 to 1000 °C) and because of the pore volume and surface area (20.35 m^2/g) achieved maximum at 1000 °C. Other researchers have described that the bamboo size (about 10 mesh to 200 mesh) had very little effect on carbon dioxide gas adsorption. However, activation temperature and KOH/C mass ratio had excellent adsorption capacity. The adsorbed amount of carbon dioxide gas (volume of micropores=0.33 to 0.82 nm, narrow micropores=0.55 nm) was 7 mmol/g (at 1 bar, 273 K).

Sulfadiazine is used to eliminate bacteria (urinary tract infections). It is an antibiotic and is available in tablet form. Several side effects could be observed, such as headache, diarrhea, nausea, numbness, and stomach pain. Magnetic bamboo-based adsorbent showed a high surface area (1388.83 m^2/g) that could be used to solve antibiotic pollution in the water environment [57]. Based on the Fourier Transform Infrared Spectroscopy (FTIR) analysis, the intensity of the C=C peak increased, indicating that the benzene ring gets involved via π-π interactions. Some peaks at 1528.68 cm^{-1} (aromatic C-H stretching or N-H bending) and 1391.47 cm^{-1} (CH_2 bending vibration) disappeared. However, Fe-O stretching vibration (Fe_3O_4) could be detected at 560.54 cm^{-1}. Adsorption data fitted well with the Langmuir model (adsorption capacity=645.08 mg/g) and pseudo-second kinetic isotherm. Thermodynamic studies revealed spontaneous (-609.7 to -805.6 kJ/mol), higher disorder and exothermic process. It was noticed that adsorption capacity increases (pH 2 to pH 4), then reduces (pH 4 to pH 6), rises slowly (pH 6 to pH 10), and finally decreases (above pH 10). When the pH was low, the presence of H^+ (acidic medium) and NH^{3+} (from the amino group) will repel each other, reducing the adsorption capacity. In contrast, strong electrostatic repulsive

forces could be observed, and a reduction in adsorption affinity happened when the pH value was too high.

Disperse dye is a synthetic dye consisting of azo groups. It has low water solubility and is free from ionizing groups. The major issue can cause allergies when contact with skin (induced dermatitis). The dispersed red 167 dye is toxic and mutagenic. It could be used in wool, fabric, silk, leather, and nylon. Response surface methodology [58] showed the highest adsorption capacity was 90.23% in the best conditions (contact time=15.4 hours, activating agent=phosphoric acid, temperature=50 °C, adsorbent dosage=12g/L, initial dye concentration=50 mg/L). In the thermodynamic investigations, the positive value of enthalpy (endothermic), positive value of entropy (increased randomness at the solid/solution interface) and negative value of free energy (spontaneous process) were described. The Acid Blue 25 (molecular weight=416.4) has a smaller molecular size and shows higher adsorption capacity [59] if compared to acid yellow 117 (molecular weight=848). The removal of dispersed orange 30 dye onto the adsorbent was studied in a fixed bed column [60]. Experimental findings confirmed that flow rate and inlet concentration increased, but bed height reduced when the breakthrough time was reduced. Experimental results showed that the maximum bed capacity was 39.97 mg/g in the specific conditions (bed height=8 cm, dye concentration=100 mg/L and the flow rate=10 mL/min).

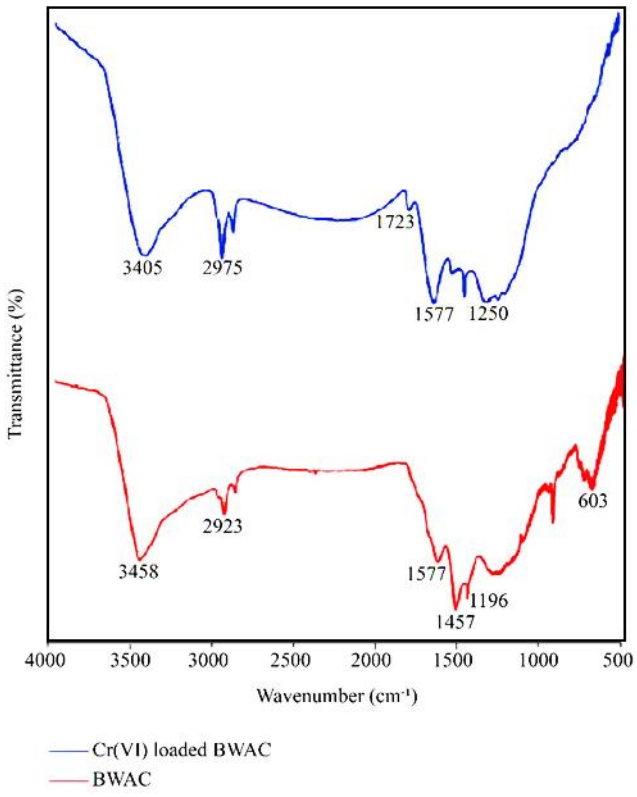

Fig. 4 Fourier transform infrared spectroscopy of the prepared activated carbon (before and after the removal of chromium) [61]

Chromium is an essential trace mineral (enhance protein, improve insulin sensitivity), consisting of trivalent chromium (safe) and hexavalent chromium (toxin). Pulmonary sensitization, sinus cancer, dermatitis and skin ulcers could result from contact with chromium. Physiochemical properties (moisture content=9.56 %, fixed carbon=73.68 %, pH=7, volatile matter=4.66 %, particle size=150μm, ash content=21.66 %) of the Oxytenanthera abyssinica [61] based activated carbon (furnace, 3 hours, KOH activation process, 1073 K) were reported. Adsorption capacity reached 98.28% at 300K and pH 2. A small shift in the frequency value could be observed after the adsorption process based on FTIR analysis (figure 4). Several peaks such as 3458 cm^{-1} (OH stretching vibration), 2923 cm^{-1} (asymmetric CH stretching), 1577 cm^{-1} (CH_2 bending), 1457 cm^{-1} (CH_3 bending), 1196 cm^{-1} (CO stretching) and 603 cm^{-1} (aliphatic alkane) could be seen. The correlation coefficient of the pseudo-first order model was 0.842, lower than pseudo second order model (R^2=0.997). The observed correlation coefficient of the Freundlich model was 0.775, higher than the Langmuir model (R^2=0.018). In the thermodynamic studies, free energy, enthalpy, and entropy values were -8.28 to -19.48 kJ/mol, -18.912 kJ/mol and 0.06614 kJ/mol.K, respectively. Humic acid's influence on chromium adsorption onto bamboo bark-based carbon was investigated [62]. Adsorption data obeyed the Freundlich model (R^2>0.99) and pseudo-second-order model (R^2>0.99) in both samples (with and without humic acid). Higher removal capacities could be seen when the pH ranged from pH 2 to pH 9, and the initial concentration increased (10 to 20 mg/L) with increasing pH value.

Bromate is a chemical compound with the formula. BrO_3^-. It could be produced in municipal drinking water. It was classified as a carcinogen that can irritate the lungs and produce headaches and impaired thinking. Activated carbon was treated with sulfuric acid and potassium permanganate to improve physico-chemical properties and adsorption capacity [63]. Experimental results highlighted that high mesopore volume and the presence of many oxygenate groups enhanced bromate adsorption. Monolayer (supported by the Langmuir model) could be observed, and the chemical sorption was dominated through intra-particle diffusion.

2.3. Bamboo-based Activated Carbon for Supercapacitor Devices

The Supercapacitor (SC) is generally classified as a hybrid capacitor, Electrical Double-Layer Capacitor (EDLCs), and pseudocapacitor. These capacitors vary due to the working mechanism in which EDLC works as a non-faradaic reaction, whereby its charge is stored at the electrode interface [64]. The EDLC is composed of two electrodes, a separator and a liquid electrolyte that works in a physical manner and does not involve any chemical reactions. The supercapacitor electrodes are commonly chosen from carbon-based material (conducting polymers and metal oxides) that possess high electronic conductivity [65]. Among the

established and emerging materials used for the electrodes are graphene, MXenes and carbon nanotube because of their high specific surface area and outstanding conductivity. The performance of EDLC is highly dependent on the electrode surface area exposed to electrolyte ions that vary between materials. The energy density at the electrode is directly proportional to its surface area. Besides, the distance between the two electrodes would also affect the energy density indirectly [66]. The strength of electrolyte solution in EDLC is always constant throughout the time of use, and its electrodes remain intact, making it capable of sustaining millions of charge/discharge cycles that lead to its long life. Therefore, the electrode materials and electrolyte selection play an important role in designing a supercapacitor that could provide rapid energy uptake and delivery and excellent performance.

Additionally, activated carbons from natural materials have been proven to prepare supercapacitor electrodes, attributed to their high specific surface area. Since the process of producing this activated carbon is quite simple and feasible, various biomaterials were chosen for this purpose, and their properties were characterized. Meanwhile, a pseudo capacitor works by using a fast Faradaic (redox reaction) process whereby the oxidation/reduction would lead to electron transfer across the electrode interface. This process could either be reversible or irreversible [67].

The pseudo capacitors demonstrated about 10–100 times higher specific capacitance value if compared to the EDLCs since they store the electrical energy faradaically in active materials [68]. Some commonly used pseudocapacitive materials to fabricate this capacitor [69] are conducting polymers (polypyrrole, polyaniline and polythiopenes) and transition metal oxides. The pseudo capacitors suffered a lack of stability due to strong redox reactions, which physically degraded the electrodes and finally resulted in low cycle life [70].

Since both EDLC and pseudo capacitors are non-ideal as they have their own advantages and disadvantages, hybrid capacitors were developed to fill the gap for both capacitors. For instance, the specific capacitance of EDLC is lower but can provide high power density and better cycling stability. Meanwhile, a pseudo capacitor possesses higher specific capacitance but lower conductivity, incurs a high cost, toxicity and poor stability [71]. Therefore, a hybrid capacitor is fabricated by combining metal oxides, conducting polymers and porous electrodes. This hybrid capacitor adopts both EDLC and pseudocapacitor mechanisms, thus enhancing its properties [72]. A wide range of materials are currently being explored for these hybrid capacitors to cater to the market demand, especially with the growing technology in smart devices. The big issue was to increase the energy densities without jeopardizing their high-power density, long cycle, and fast charging/discharging. Therefore, electrode materials are thoroughly explored, and the selection of electrolytes was carefully done [73]. Opening voltage, energy density value, and power density value were found to be up to 3.5 V, 3-5 Wh/kg & 900-10000W/kg, up to 2.3 V, 1-10 Wh/kg & 500-5000 W/kg, 3.8-19V, 8-80 Wh/kg & 200-1500 W/Kg in EDLC, pseudocapacitor and hybrid capacitor, respectively. With reference to its outstanding properties and the growing demand for smart technology, research on the fabrication of supercapacitors is extensively explored as the development of supercapacitors is practical in various energy storage applications. One of the crucial areas is to serve as a backup power supply in the case of power disruptions [74]. Table 1 highlights some limitations and advantages of supercapacitors.

Table 1. Advantages and limitations of supercapacitors

Advantages	The supercapacitors have very little degradation over thousands of charge cycles, making them more favorable to be chosen as an energy storage device.
	Supercapacitors have a high number of charge-discharge cycles (thousands or millions) compared to conventional rechargeable batteries. This would enable it to last for the entire time of most devices.
	High-performance reliability with higher charging rates.
	The supercapacitors can easily be connected in series to provide higher voltages for devices that require high power input.
	In terms of safety, supercapacitors are considered safe and practical since there are no corrosive electrolytes and the materials used are of low toxicity.
	Its small size and lightweight properties make it viable for installation in small areas/devices.
	Easy maintenance
Limitations	Has the highest dielectric absorption in comparison with other types of capacitors.
	Since it has very low internal resistance, extremely rapid discharge occurs when shorted, leading to spark hazards.
	High discharge rate is reported to be higher than that of an electrochemical battery.
	Low maximum voltage limit. Hence, a series of connections is required to obtain higher voltages.
	Low energy density

Since supercapacitors form a bridge between conventional capacitors and batteries, research works have been extensively conducted since the last decade to improvise and enhance the performance of supercapacitors while tailoring their disadvantages to fit the desired applications in various fields better. Some points are worth taking into consideration in order to develop a compact and high-performance supercapacitor for advanced technology.

Monolith form (binder-free electrode) activated carbon has been synthesized using bamboo stem wastes via zinc chloride activation, carbonization process and physical activation [75]. In the carbonization process (600 °C), light tar, organic acids and volatile content have been reduced successfully. As a result, the prepared samples' diameter, mass, and thickness were also reduced. In the physical activation process (carbon dioxide atmosphere), non-carbon content has been removed and developed as initial pores. Experimental results revealed that combining mesopores and micropores could enhance the diffusion of electrolyte ions. Micropores improved surface area, while mesopores showed smooth ion transport pathways. One-step zinc chloride impregnation indicated the highest specific capacitance (154 F/g, 0.2 mm thickness, 1mV/s of scan rate) if compared to two-step (132 F/g) and three-step impregnation (131 F/g).

Potassium hydroxide was used [76] as an activation agent that could produce a higher surface area (3000 m^2/g). It was noted that these carbons offered excellent power density, specific capacitance, and energy density. Also, high cyclic stability could be detected, and the specific capacitance retention reached 91% (after 3000 cycles) based on the experimental results.

Zawawi and co-workers [77] have demonstrated the production of bamboo-based activated carbon in specific conditions (activating agent=potassium hydroxide, carbonization temperature=800 °C, microwave power intensities=100, 300 and 500 W, ultrasonic soaking time= 60 minutes). Proximate analysis, ultimate analysis, surface area and total pore volume were studied (Table 2). Higher surface area could be observed in the activated carbon prepared using 100 W (BAC A) if compared to 300 W (BAC B) and 500 W (BAC C) because of the opening of restricted pores and higher carbonization temperature. The yield percentage will decline if the carbon has a high amount of volatile matter. Also, low inorganic content is needed to form high fixed carbon content and low ash content. In the FTIR analysis, ketones, lactones, carboxylic acid, aromatic rings, and anhydrides are presented in the bamboo-based activated carbon. Based on the electrochemical properties, specific capacitance reached 77 F/g (scan rate=25 mV/s) in 1 mol/L KOH electrolyte. Also, the capacitance was reduced (76 F/g to 67 F/g) when the scan rate was increased (50 mV/s to 150 mV/s) because the penetration of ions (into mesopores) will be limited when the scar rate increases.

Table 2. Ultimate analysis, proximate analysis, surface area and the porosity of the prepared activated carbon [77]

	A	B	C
Surface area (m^2/g)	646.87	612.52	607.41
Total pore volume (cm^3/g)	0.28	0.39	0.26
Moisture content (%)	0.4	44	12.4
Volatile content (%)	7.2	6.7	6.9
Ash content (%)	46.8	27.5	26.9
Fixed carbon (%)	45.6	27.5	26.9
Ultimate analysis: Oxygen Hydrogen Carbon	13.53 3.05 83.42	18.85 3.65 77.5	35.36 1.12 63.52

Moso bamboo was employed [78] to produce activated carbon (nitrogen and carbon dioxide gas atmosphere, gas flow rate=0.5L/min, carbonized temperature=750 to 900 °C). As shown in the TG/DTG analysis, three sub-processes happened during the pyrolysis stage, namely dehydration (room temperature to 125 °C), devolatilization (200 °C to 450 °C) and char formation (more than 450 °C). It was noted that ash could speed up the reaction, increase yield percentage, and enhance the tar reduction. Raman spectra confirmed that the carbonization temperature and carbon dioxide activation have not influenced the graphitic structures and layers. The energy density and specific capacitance were found to be 7.8 Wh/g and 160 F/g, respectively. These electrodes showed good stability (virtually constant capacitance after 10000 cycles).

Bamboo powder [79] has been used to produce activated carbon in the mentioned conditions (ratio of bamboo/$KMnO_4$=1:4, nitrogen atmosphere, 800 °C, 120 minutes, heating rate=5 °C/min). Based on the TEM images, a well-developed structure with small pores (<20 nm) could be observed in the obtained activated carbon. EDX analysis confirmed 89% carbon and 10% oxygen in the prepared carbons. BET-specific surface area (915 m^2/g) and total pore volume (1.05 cm^3/g) have been described. It was noted that the volume of macroporous and mesoporous increased in the $KMnO_4$ activation process according to the pore size distribution curves. In the FTIR studies, several peaks at 3400 cm^{-1} (OH stretching of hydroxyl, carboxyl), 1600 cm^{-1} (C=C bonds), 1720 cm^{-1} (C=O bonds) and 1000-1450 cm^{-1} (C-O bonds) could be identified. $KMnO_4$ is a strong oxidizing agent that could enhance the production of oxygen-containing groups. The cyclic voltammetry curves (figure 5) indicated well symmetric rectangular shape (broaden humps), indicating properties of electrochemical double-layer capacitance). The capacitance reduces when the scan rate increases from 2 mV/s (225 F/g) to 100 mV/s (30 F/g).

Mesoporous-activated carbon [80] has been synthesized through steam activation and carbonization. Mesopore ratio, specific surface area and yield were 7.5%-44.5%, 960-2700 m^2/g, and 4.6%-22.9%, respectively.

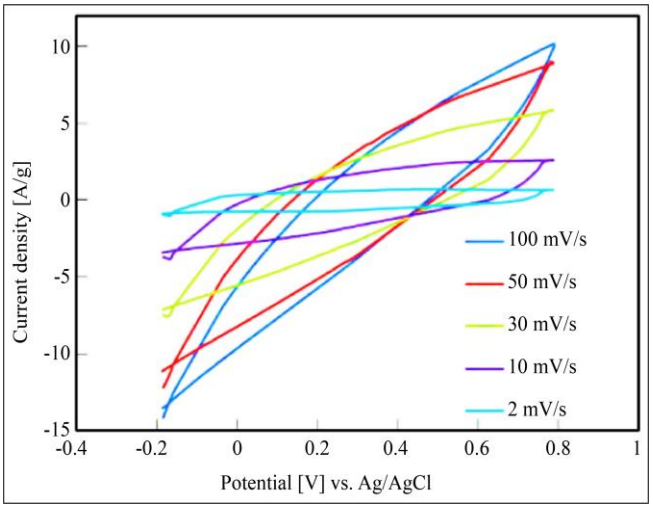

Fig. 5 The cyclic voltammetry curves of the activated carbon-based electrode at different potential scan rates [79]

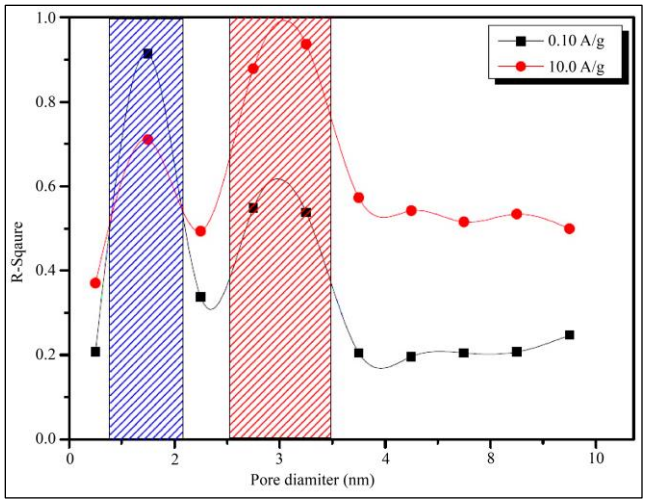

Fig. 6 Correlation between the pore volume and specific capacitance [80]

Pore size distribution reflects that the micropore volume increased via pore deepening, while the mesopore volume increased through the pore drilling process. It was noted that raw material consisted of big amounts of ash. However, a lower amount could be seen in the prepared activated carbon due to the phosphoric acid stabilization process (ash was removed). In the SEM studies, more relatively densely could be seen when the activation time was short because of high apparent density.

Figure 6 indicates a higher corelation (R^2=0.9) at a current density of 0.1 A/g and pore diameter of 0.15 nm. However, micropore and mesopore (widths between 3.5 and 4.5 nm) regions were detected when the current density was 10 A/g. Specific capacitance was 86.7 F/g (steam activation for 1 hour and 900 °C). Based on Table 3, many researchers have synthesized the activated carbon using bamboo. Research findings and specific experimental conditions have also been described.

Table 3. Experimental conditions and research findings in bamboo-based activated carbon

References	Experimental conditions and Research findings
Tian et al., 2015	• Beehive-like hierarchy with nanoporous materials prepared via the bio-inspired method showed a large surface area (1472 m^2/g) and excellent electronic conductivity (4.5 S/cm). • Enhanced power density was 42000 W/kg at high energy density (43.3 Wh/kg) could be observed in ionic liquid electrolyte systems [81].
Kim et al., 2006	• Carbonization and activation (with non-aqueous electrolyte solution and steam) were used to produce carbon. • The capacitances (5 F/g to 60 F/g) and specific surface area (445 m^2/g to 1025 m^2/g) strongly depended on the activation conditions. • The best activation conditions [82] were observed (activation time=60 minutes, activation temperature=900 °C). [82].
Huang et al., 2015	• MnO_2 (size=16.92 nm) was loaded on the carbon surface. • A large specific capacitance value (221.45 F/g) could be observed (current density=1 A/g). • 89.29% retention (after 1000 cycles) could be seen, representing good cycling stability [83].
Syed et al., 2022	• High surface area and multi-porous structures could be seen in SiC and nitrogen-based doped activated carbon [84]. • Excellent capacitive properties (369 F/g at 0.5 A/g) could be seen after 5000 charge-discharge cycles (100% retention).
Xinhong et al., 2012	• High-performance conducting polymer (polyaniline)--activated carbon (carbonized from bamboo) was synthesized [85]. • 92% of capacitance was successfully retained (after 1000 cycles). • Energy density was 47.5 Wh/kg.
Camila et al. 2016	• Specific capacity = 510 F/g (at 0.4 A/g), energy density = 54 Wh/kg [86]. • The obtained carbonized bamboo fibers indicate excellent stable performance over 5000 charge and recharge cycles. • The supercapacitor device performance has been improved at 70 °C (about 65%) if compared to 10 °C.

Xiufang et al., 2017	• Nitrogen-doped carbon materials showed a large specific surface area (972 m^2/g) and interconnected porous framework [87]. • Long cycling life stability with excellent capacitance (412 F/g in KOH electrolyte).
Montoya et al., 2017	• Guadua angustifolia Kunth was used as a precursor to produce activated carbon via KOH (surface area=309 m^2/g) and NaOH (surface area=408 m^2/g) activation process [88]. • The highest capacitance was 0.92 F using 0.5V (fixed value in bias voltage).
Xu et al., 2021	• Iron-doped porous activated carbon indicated spherical morphology and high surface area (1509.5 m^2/g) [89]. • The introduced iron oxide gives extra pseudocapacitance, showing an excellent capacitance value (467 F/g at 0.5 A/g).
Hao et al., 2015	• Energy density, specific capacitance and electrochemical cycling stability were improved in the boron and nitrogen KOH-activated carbon [90].
Pang et al., 2022	• Hierarchical pores, three-dimensional conductive network structure and high heteroatom doping (8.43%) could be observed using green cellulose solvent [91]. • Good cyclic stability, excellent capacitive performance (280 F/g at 0.3 A/g) and good rate capability were detected.
Xi et al., 2018	• Formation of porous nanoplatelets wrapped carbon aerogel using urea/sodium hydroxide solution (to dissolve bamboo cellulose fibre). • The obtained carbon showed great flexibility (86%, stress of 23 kPa) and high surface area [92]. • Specific capacitance was 381 F/g in 6M KOH solution.
Farma et al., 2021	• Highly porous materials were synthesized [93] • Surface area=1137.86 m^2/g, specific capacitance=174 F/g (carbonization temperature=800 °C).
Jayachandran et al., 2021	• Bamboo leaf [94] based activated carbon was synthesized via carbonization (120 minutes, 500 °C) and chemical activation (KOH). • Specific capacitance successfully reached 290 F/g (at 1 A/g) using mixed electrolyte (0.5M KOH + 1M Na_2SO_4). • Capacity retention was 93% (after achieving 1000 cycles) at 10 A/g.
Guoxiong et al., 2018	• Properties (porosity=mesoporous structure, rate capability=193.8 F/g at 20 A/g, surface area=2221 m^2/g, capacitance value=293 F/g (0.5 A/g, 3M KOH), energy density=10.9 Wh/kg, power density=63 W/kg) of the product when the activation temperature was 900 °C have been highlighted [95].
Ajay and Dinesh, 2021	• In BET studies, surface area, average diameter, and pore volume were 1273 m^2/g, 1.92 nm and 0.6119 cm^3/g, respectively, in the obtained carbon (nitrogen atmosphere, KOH activating agent, 120 minutes, 800 °C). • Specific capacitance reached 143 F/g (5mV scan rate) in 1 M KOH electrolyte [96]. • Efficiency retention was successfully reduced (70%) after 25000 cycles according to the Galvanic Charge Discharge analysis.
Linlin et al., 2020	• Nitrogen, sulphur co-doped bamboo fiber carbon [97] was synthesized (thiourea=dopant, $K_3Fe(CN)_6$=graphitization catalysis). • Specific capacitance=328 F/g, acceptable rate capability=61.3 %, at 15 A/g (three electrode system).
Gege et al., 2019	• Bamboo shoot shell-based N-doped carbon was produced (carbonization, KOH activation process) [98]. • Properties (surface area=3300 m^2/g, mesoporous=2.8 nm) of the products were described. • Capacitance reached 209 F/g (6 M KOH, 0.5 A/g) and remained (188 F/g) when high current density (10 A/g) was applied. • Capacity retention=95 % after 10000 cycles (at 10 A/g)
Qiushi et al., 2019	• Manganese silicate hybridized carbon materials (precursor was bamboo leaves) were prepared [99]. • Capacitance achieved 162.2 F/g (current density=0.5 A/g), and capacitance retention was 85 % (after 10000 cycles)
Shengli et al., 2011	• Activated carbon was prepared using a microwave heating process and showed excellent cycling performance and charge/discharge properties [100]. • Specific capacitance was 277.46 F/g (microwave power=720 W, microwave radiation time=12 minutes, KOH to bamboo impregnation=6:1)

3. Conclusion

Activated carbon prepared using bamboo showed excellent porosity structure, large surface area, and desired surface functionalization. In this work, heavy metals, dye, pollutant gases, antibiotics, and organic compounds have been successfully removed. The Langmuir model or Freundlich

isotherm was well matched with adsorption data. This product type has also been broadly employed in the electrochemical industry (supercapacitor electrodes). The prepared carbon indicated great porous microstructure and high absorption capacity. These properties make it appropriate for the adsorption/desorption of electrolyte ions in non-Faradaic processes without involving chemical reactions. Experimental findings confirmed that the activation process affected the electrochemical performance of activated carbon electrodes.

Acknowledgments

INTI International University, Malaysia (HO SM) financially supported this research work.

References

[1] S. Kyrii, M. Zakhar, and D. Tetiana, "Impact of Modification by Red Mud Components on the Sorption Properties of Activated Carbon," *Applied Surface Science Advances*, 2023. [CrossRef] [Google Scholar] [Publisher Link]

[2] Jianbin Wang et al., "Prediction of the Ash Melting Behavior and Mineral Phase Transformation during the Co-Gasification of Waste Activated Carbon and Coal Water Slurry," *Fuel*, vol. 340, 2023. [CrossRef] [Google Scholar] [Publisher Link]

[3] Omaima A. Hussain et al., "Preparation and Characterization of Activated Carbon from Agricultural Wastes and their Ability to Remove Chlorpyrifos from Water," *Toxicology Reports*, vol. 10, pp. 146-154, 2023. [CrossRef] [Google Scholar] [Publisher Link]

[4] Sergey N. Maximoff et al., "Performance Evaluation of Activated Carbon Sorbents for Indoor Air Purification during Normal and Wildfire Events," *Chemosphere*, vol. 304, 2022. [CrossRef] [Google Scholar] [Publisher Link]

[5] Xiao Wang et al., "Cation-Π Interaction in $Mg(OH)_2$@GO-Coated Activated Carbon Fiber Cloth for Rapid Removal and Recovery of Divalent Metal Cations by Flow-Through Adsorption," *Resources, Conservation and Recycling*, vol. 188, 2023. [CrossRef] [Google Scholar] [Publisher Link]

[6] Mohamed Chaker Ncibi, and Mika Sillanpää, "Optimizing the Removal of Pharmaceutical Drugs Carbamazepine and Dorzolamide from Aqueous Solutions using Mesoporous Activated Carbons and Multi-Walled Carbon Nanotubes," *Journal of Molecular Liquids*, vol. 238, pp. 379-388, 2017. [CrossRef] [Google Scholar] [Publisher Link]

[7] Zoha Heidarinejad et al., "Methods for Preparation and Activation of Activated Carbon: A Review," *Environmental Chemistry Lertters*, vol. 18, pp. 393–415, 2020. [CrossRef] [Google Scholar] [Publisher Link]

[8] Kingdom Kponanyie Dune et al., "Production, Activation and Characterisation of PKS-Biochar from Elaeis Guineensis Biomass activated with HCl for Optimum Produced Water Treatment," *International Journal of Recent Engineering Science*, vol. 9, no. 1, pp. 1-7, 2022. [CrossRef] [Google Scholar] [Publisher Link]

[9] Soonmin Ho, and Mohamad Jani Saad, "A Review on Heavy Metal and Dye Removal via Activated Carbon Adsorption Process," *Asian Journal of Chemistry*, vol. 35, no. 1, pp. 1-16, 2023. [CrossRef] [Publisher Link]

[10] Soonmin Ho, "Low-Cost Adsorbents for the Removal of Phenol/Phenolics, Pesticides, and Dyes from Wastewater Systems: A Review," *Water*, vol. 14, no. 20, pp. 1-37, 2022. [CrossRef] [Google Scholar] [Publisher Link]

[11] Wen-Pei Low et al., "Adsorption of Zinc, Copper, and Iron from Synthetic Wastewater using Watermelon (Citrullus Lanatus), Mango (Mangifera Indica L), and Rambutan Peels (Nephelium Lappaceum L) as Biosorbents," *Journal of Engineering Science and Technology*, vol. 18, no. 1, pp. 386-405, 2023. [Google Scholar] [Publisher Link]

[12] A.W. Samsuri, F. Sadegh-Zadeh, and B.J. Seh-Bardan, "Characterization of Biochars Produced from Oil Palm and Rice Husks and their Adsorption Capacities for Heavy Metals," *International Journal of Environmental Science and Technology*, vol. 11, pp. 967–976, 2014. [CrossRef] [Google Scholar] [Publisher Link]

[13] Made Sucipta et al., "Development of Respirator Design for Children Using Bamboo-Based Activated Carbon Filter and Bipolar Ionization," *Alexandria Engineering Journal*, vol. 63, pp. 527-547, 2023. [CrossRef] [Google Scholar] [Publisher Link]

[14] Chaomin Duan et al., "Performance and Characterization of Bamboo-Based Activated Carbon Prepared by Boric Acid Activation," *Materials Chemistry and Physics*, vol. 295, 2023. [CrossRef] [Google Scholar] [Publisher Link]

[15] Yao Xia et al., "Preparation of Multi-Layered Microcapsule-Shaped Activated Biomass Carbon with Ultrahigh Surface Area from Bamboo Parenchyma Cells for Energy Storage and Cationic Dyes Removal," *Journal of Cleaner Production*, vol. 396, 2023. [CrossRef] [Google Scholar] [Publisher Link]

[16] N. Jayarambabu et al., "Bamboo-Mediated Silver Nanoparticles Functionalized with Activated Carbon and their Application for Non-Enzymatic Glucose Sensing," *Inorganic Chemistry Communications*, vol. 147, 2023. [CrossRef] [Google Scholar] [Publisher Link]

[17] Ganmao Su et al., "Gaseous Formaldehyde Adsorption by Eco-Friendly, Porous Bamboo Carbon Microfibers Obtained by Steam Explosion, Carbonization, and Plasma Activation," *Chemical Engineering Journal*, 2023. [CrossRef] [Google Scholar] [Publisher Link]

[18] Huisheng Peng et al., *Polymer Materials for Energy and Electronic Applications*, 1st ed., Academic Press: London, 2017. [Google Scholar] [Publisher Link]

[19] Waseem Raza et al., "Recent Advancements in Supercapacitor Technology," *Nano Energy*, vol. 52, pp. 441–473, 2018. [CrossRef] [Google Scholar] [Publisher Link]

[20] Nesrine Abderrahim et al., "Optimization of Microwave Assisted Synthesis of Activated Carbon from Biomass Waste for Sustainable Industrial Crude Wet-Phosphoric Acid Purification," *Journal of Cleaner Production*, vol. 394, 2023. [CrossRef] [Google Scholar] [Publisher Link]

[21] Stanley E. Ngene, and Kiran Tota-Maharaj, "Effectiveness of Sand Filtration and Activated Carbon in Oilfield Wastewater Treatment," *SSRG International Journal of Chemical Engineering Research*, vol. 7, no. 2, pp. 13-23, 2020. [CrossRef] [Google Scholar] [Publisher Link]

[22] Jianzhong Zhu et al., "Production, Characterization and Properties of Chloridized Mesoporous Activated Carbon from Waste Tyres," *Waste Management and Research*, vol. 27, no. 6, pp. 553–560, 2009. [CrossRef] [Google Scholar] [Publisher Link]

[23] M. Kini Srinivas et al., "Adsorption of Basic Dye from Aqueous Solution Using HCL Treated Saw Dust (Lagerstroemia Microcarpa): Kinetic, Modeling of Equilibrium, Thermodynamic, INDIA," *International Research Journal of Environmental Sciences*, vol. 2, no. 8, pp. 6-16, 2013. [Google Scholar] [Publisher Link]

[24] Titus M. Kasimu, Harun M. Mbuvi, and Francis M. Maingi, "Evaluation of Activated Charcoal Based Hydrogels Functionalized with Maleic Acid on Growth Performance of Zea Mays in Semi-arid Regions of Kenya," *SSRG International Journal of Agriculture and Environmental Science*, vol. 9, no. 3, pp. 69-76, 2022. [CrossRef] [Google Scholar] [Publisher Link]

[25] N. Rambabu et al., "Production, Characterization, and Evaluation of Activated Carbons from De-Oiled Canola Meal for Environmental Applications," *Industrial Crops and Products*, vol. 65, pp. 572–581, 2015. [CrossRef] [Google Scholar] [Publisher Link]

[26] Juan Yang, and Keqiang Qiu, "Preparation of Activated Carbons from Walnut Shells via Vacuum Chemical Activation and their Application for Methylene Blue Removal," *Chemical Engineering Journal*, vol. 165, pp. 209–217, 2010. [CrossRef] [Google Scholar] [Publisher Link]

[27] Zohra Belala et al., "Biosorption of Copper from Aqueous Solutions by Date Stones and Palm-Trees Waste," *Environmental Chemistry Letters*, vol. 9, pp. 65–69, 2011. [CrossRef] [Google Scholar] [Publisher Link]

[28] Pratibha R. Gawande, Jayant P. Kaware, "Review on- Study of Characteristics of Low Cost Activated Carbon," *SSRG International Journal of Chemical Engineering Research*, vol. 4, no. 2, pp. 6-9, 2017. [CrossRef] [Publisher Link]

[29] S.M.A. Mahanim et al., "Production of Activated Carbon from Industrial Bamboo Wastes," *Journal of Topical Forest Science*, vol. 23, no. 4, pp. 417–424, 2011. [Google Scholar] [Publisher Link]

[30] Şakir Yılmaz, Ümit Ecer, and Tekin Şahan, "Synthesis, Characterization and Application of Iron-Supported Activated Carbon Derived from Aloe Vera Leaves to Improve Anaerobic Digestion of Food Waste: An Optimization Approach," *Journal of Environmental Chemical Engineering*, vol. 11, no. 5, 2023. [CrossRef] [Google Scholar] [Publisher Link]

[31] Niyaz Mohammad Mahmoodi et al., "Novel Magnetic Amine Functionalized Carbon Nanotube/Metal-Organic Framework Nanocomposites: From Green Ultrasound-Assisted Synthesis to Detailed Selective Pollutant Removal Modelling from Binary Systems," *Journal of Hazardous Materials*, vol. 368, pp. 746–759, 2019. [CrossRef] [Google Scholar] [Publisher Link]

[32] Jie He et al., "Activated Carbon Modified Titanium Dioxide/Bismuth Trioxide Adsorbent: One-Pot Synthesis, High Removal Efficiency of Organic Pollutants, and Good Recyclability," *Journal of Colloid and Interface Science*, vol. 648, pp. 1034-1043, 2023. [CrossRef] [Google Scholar] [Publisher Link]

[33] Ahmed M. Zayed et al., "Facile Synthesis of Eco-Friendly Activated Carbon from Leaves of Sugar Beet Waste as a Superior Nonconventional Adsorbent for Anionic and Cationic Dyes from Aqueous Solutions," *Arabian Journal of Chemistry*, vol. 16, no. 8, 2023. [CrossRef] [Google Scholar] [Publisher Link]

[34] Goldi Sharma, and S. Kamalesu, "Review on Sustainable Synthesis of Semi-Amorphous Ti-BDS MOF Material, Activated Carbon, and Graphene," *Materials Today Proceedings*, 2023. [CrossRef] [Google Scholar] [Publisher Link]

[35] Meghdad Pirsaheb et al., "Green Synthesis and Characterization of Sno_2, Cuo, Fe_2O_3/Activated Carbon Nanocomposites and their Application in Electrochemical Hydrogen Storage," *International Journal of Hydrogen Energy*, vol. 48, no. 16, pp. 23594-23606, 2023. [CrossRef] [Google Scholar] [Publisher Link]

[36] Nurul Najihah Binti Rosli et al., "Ruthenium Dye (N3) Removal from Simulated Wastewater Using Bamboo Charcoal and Activated Bamboo Charcoal," *Key Engineering Materials*, vol. 765, pp. 92-98, 2018. [CrossRef] [Google Scholar] [Publisher Link]

[37] Abu Masanizan et al., "The Removal of Ruthenium-Based Complexes N3 Dye from DSSC Wastewater Using Copper Impregnated KOH-Activated Bamboo Charcoal," *Water, Air & Soil Pollution*, 2021. [CrossRef] [Google Scholar] [Publisher Link]

[38] Y.X. Wang, H.H. Ngo, and W.S. Guo, "Preparation of a Specific Bamboo Based Activated Carbon and Its Application for Ciprofloxacin Removal," *Science of the Total Environment*, vol. 533, pp. 32-39, 2015. [CrossRef] [Google Scholar] [Publisher Link]

[39] Xiaoming Peng et al., "Amine-Functionalized Magnetic Bamboo-Based Activated Carbon Adsorptive Removal of Ciprofloxacin and Norfloxacin: A Batch and Fixed-Bed Column Study," *Bioresource Technology*, vol. 249, pp. 924-934, 2018. [CrossRef] [Google Scholar] [Publisher Link]

[40] Xiaoming Peng et al., "Adsorption Behavior and Mechanisms of Ciprofloxacin from Aqueous Solution by Ordered Mesoporous Carbon and Bamboo-Based Carbon," *Journal of Colloid Interface Science*, vol. 460, pp. 349-360, 2015. [CrossRef] [Google Scholar] [Publisher Link]

[41] N.U. Udeh, and J.C. Agunwamba, "Removal of Heavy Metals from Aqueous Solution Using Bamboo Based Activated Carbon," *International Journal of Engineering Invention,* vol. 6, no. 2, pp. 1-12, 2017. [Google Scholar] [Publisher Link]

[42] Jherwin Ocreto et al., "Competitive Effects for the Adsorption of Copper, Cadmium and Lead Ions Using Modified Activated Carbon from Bamboo," *MATEC Web of Conferences,* 2019. [CrossRef] [Google Scholar] [Publisher Link]

[43] Chaomin Duan et al., "Absorptivity and Kinetics for Low Concentration of Gaseous Formaldehyde on Bamboo-Based Activated Carbon Loaded with Ammonium Acetate Particles," *Environmental Research,* vol. 222, 2023. [CrossRef] [Google Scholar] [Publisher Link]

[44] W.D.P. Rengga, M. Sudibandriyo, and M. Nasikin, "Adsorption of Low-Concentration Formaldehyde from Air by Silver and Copper Nano-Particles Attached on Bamboo-Based Activated Carbon," *International Journal of Chemical Engineering and Applications,* vol. 4, pp. 332-336, 2013. [CrossRef] [Google Scholar] [Publisher Link]

[45] Wara Dyah Pita Rengga et al., "Silver Nanoparticles Deposited on Bamboo-Based Activated Carbon for Removal of Formaldehyde," *Journal of Environmental Chemical Engineering,* vol. 5, no. 2, pp. 1657-1665, 2017. [CrossRef] [Google Scholar] [Publisher Link]

[46] Wara Dyah Pita Rengga, Sri Wahyuni, and Agung Feinnudin, "Thermodynamics of Formaldehyde Removal by Adsorption onto Nanosilver Loaded Bamboo-Based Activated Carbon," *Materials Science Forum,* vol. 890, pp. 93-97, 2017. [CrossRef] [Google Scholar] [Publisher Link]

[47] Wenxiang Jing et al., "One-Pot Method to Synthesize Silver Nanoparticle-Modified Bamboo-Based Carbon Aerogels for Formaldehyde Removal," *Polymers,* vol. 14, no. 5, 2022. [CrossRef] [Google Scholar] [Publisher Link]

[48] Gregório Mateus Santana et al., "Activated Carbon from Bamboo (Bambusa Vulgaris) for Methylene Blue Removal: Prediction to the Environment Applications," *Ciência Florestal,* vol. 28, no. 3, pp. 1179-1191, 2018. [CrossRef] [Google Scholar] [Publisher Link]

[49] Qing-Song Liu et al., "Modification of Bamboo-Based Activated Carbon using Microwave Radiation and Its Effects on the Adsorption of Methylene Blue," *Applied Surface Science,* vol. 256, no. 10, pp. 3309-3315, 2010. [CrossRef] [Google Scholar] [Publisher Link]

[50] B.H. Hameed, A.T.M. Din, and A.L. Ahmad, "Adsorption of Methylene Blue onto Bamboo-Based Activated Carbon: Kinetics and Equilibrium Studies," *Journal of Hazardous Materials,* vol. 141, no. 3, pp. 819-825, 2007. [CrossRef] [Google Scholar] [Publisher Link]

[51] Xinxin Ma et al., "Preparation of High-Performance Activated Carbons using Bamboo through One Step Pyrolysis," *BioResources,* vol. 14, no. 1, pp. 688-699, 2019. [Google Scholar] [Publisher Link]

[52] Khaizuran Fyrdaus Azlan Zahari et al., "Mesoporous Activated Carbon from Bamboo Waste via Microwave-Assisted K_2CO_3 Activation: Adsorption Optimization and Mechanism for Methylene Blue Dye," *Separations,* vol. 9, no. 12, pp. 1-19, 2022. [CrossRef] [Google Scholar] [Publisher Link]

[53] Changqing Su et al., "Vocs Adsorption of Resin-Based Activated Carbon and Bamboo Char: Porous Characterization and Nitrogen-Doped Effect," *Colloids Surfaces A: Physicochemical and Engineering Aspects,* vol. 601, 2020. [CrossRef] [Google Scholar] [Publisher Link]

[54] Lijuan Hu et al., "Monolithic Bamboo-Based Activated Carbons for Dynamic Adsorption of Toluene," *Journal of Porous Materials*, vol. 24, pp. 541–549, 2017. [CrossRef] [Google Scholar] [Publisher Link]

[55] Weijun Ying et al., "In Situ Dry Chemical Synthesis of Nitrogen-Doped Activated Carbon from Bamboo Charcoal for Carbon Dioxide Adsorption," *Materials,* vol. 15, no. 3, pp. 1-12, 2022. [CrossRef] [Google Scholar] [Publisher Link]

[56] Pei-Hsing Huang et al., "Effects of Carbonization Parameters of Moso-Bamboo-Based Porous Charcoal on Capturing Carbon Dioxide," *The Scientific World Journal*, 2014. [CrossRef] [Google Scholar] [Publisher Link]

[57] Fan Yang et al., "Bamboo-Based Magnetic Activated Carbon for Efficient Removal of Sulfadiazine: Application and Adsorption Mechanism," *Chemosphere,* vol. 323, 2023. [CrossRef] [Google Scholar] [Publisher Link]

[58] Lianggui Wang, "Removal of Disperse Red Dye by Bamboo-Based Activated Carbon: Optimisation, Kinetics and Equilibrium," *Environmental Science and Pollution Research,* vol. 20, pp. 4635–4646, 2013. [CrossRef] [Google Scholar] [Publisher Link]

[59] L.S. Chan, W.H. Cheung, and G. McKay, "Adsorption of Acid Dyes by Bamboo Derived Activated Carbon," *Desalination,* vol. 218, no. 1-3, pp. 304-312, 2008. [CrossRef] [Google Scholar] [Publisher Link]

[60] A.A. Ahmad, A. Idris, and B.H. Hameed, "Modelling of Disperse Dye Adsorption onto Bamboo Based Activated Carbon in Fixed Bed Column," *Desalination and Water Treatment,* vol. 52, no. 1-3, pp. 248-256, 2014. [CrossRef] [Google Scholar] [Publisher Link]

[61] Tamirat Dula, Khalid Siraj, and Shimeles Addisu Kitte, "Adsorption of Hexavalent Chromium from Aqueous Solution Using Chemically Activated Carbon Prepared from Locally Available Waste of Bamboo (Oxytenanthera abyssinica)," *ISRN Environmental Chemistry,* 2014. [CrossRef] [Google Scholar] [Publisher Link]

[62] Yan-Juan Zhang et al., "Adsorption of Cr (VI) on Bamboo Bark-Based Activated Carbon in the Absence and Presence of Humic Acid," *Colloids and Surfaces A: Physicochemical and Engineering Aspects*, vol. 481, pp. 108-116, 2015. [CrossRef] [Google Scholar] [Publisher Link]

[63] Ho-Wen Chen et al., "Adsorption Characteristics of Trace Levels of Bromate in Drinking Water by Modified Bamboo-Based Activated Carbons," *Journal of Environmental Science and Health, Part A,* vol. 52, no. 11, pp. 1055-1062, 2017. [CrossRef] [Google Scholar] [Publisher Link]

[64] Rafael Vicentini et al., "How to Measure and Calculate Equivalent Series Resistance of Electric Double-Layer Capacitors," *Molecules*, vol. 24, no. 8, pp. 1-9, 2019. [CrossRef] [Google Scholar] [Publisher Link]

[65] Linpo Yu, and George Z. Chen, "Redox Electrode Materials for Supercapatteries," *Journal of Power Sources*, vol. 326, pp. 604–612, 2016. [CrossRef] [Google Scholar] [Publisher Link]

[66] Xiaoyu Shi et al., "Recent Advances of Graphene-Based Materials for High-Performance and New-Concept Supercapacitors," *Journal of Energy Chemistry*, vol. 27, no. 1, pp. 25–42, 2018. [CrossRef] [Google Scholar] [Publisher Link]

[67] Waseem Raza et al., "Recent Advancements in Supercapacitor Technology," *Nano Energy*, vol. 52, pp. 441–473, 2018. [CrossRef] [Google Scholar] [Publisher Link]

[68] Indrajit Shown et al., "Conducting Polymer-Based Flexible Supercapacitor," *Energy Science & Engineering*, vol. 3, no. 1, pp. 2–26, 2015. [CrossRef] [Google Scholar] [Publisher Link]

[69] Lei Zhou et al., "Metal Oxides in Supercapacitors," *Metal Oxides in Energy Technologies*, pp. 169-203, 2018. [CrossRef] [Google Scholar] [Publisher Link]

[70] Yuqi Jiang, and Jinping Liu, "Definitions of Pseudocapacitive Materials: A Brief Review," *Energy & Environmental Materials*, vol. 2, no. 1, pp. 30–37, 2019. [CrossRef] [Google Scholar] [Publisher Link]

[71] Karim Khan et al., "Going Green with Batteries and Supercapacitor: Two Dimensional Materials and their Nanocomposites Based Energy Storage Applications," *Progress in Solid State Chemistry*, vol. 58, 2020. [CrossRef] [Google Scholar] [Publisher Link]

[72] Angélica M. Baena-Moncada et al., "Advances in the Design and Application of Transition Metal Oxide-Based Supercapacitors," *Open Chemistry*, 2021. [CrossRef] [Google Scholar] [Publisher Link]

[73] Mulumudi Rajesh, and A. Lakshmi Devi, "Wind, PV Solar, Hydro and Hybrid Energy Storage System-Based Intelligent Adaptive Control for Standalone Distributed Generation System," *SSRG International Journal of Electrical and Electronics Engineering*, vol. 9, no. 11, pp. 67-94, 2022. [CrossRef] [Publisher Link]

[74] Patrice Simon, Yury Gogotsi, and Bruce Dunn, "Where do Batteries End and Supercapacitors Begin?," *Science*, vol. 343, pp. 1210–1211, 2014. [CrossRef] [Google Scholar] [Publisher Link]

[75] Erman Taer et al., "Bamboo-Based Activated Carbon as Binder-Free Electrode of Supercapacitor Application," *Journal of Physics: Conference Series*, 2020. [CrossRef] [Google Scholar] [Publisher Link]

[76] Cheol-Soo Yang , Yun Su Jang , and Hae Kyung Jeong, "Bamboo-Based Activated Carbon for Supercapacitor Applications," *Current Applied Physics*, vol. 14, no. 12, pp. 1616-1620, 2014. [CrossRef] [Google Scholar] [Publisher Link]

[77] Norakmalah Mohd Zawawi et al., "Chemical and Electrochemical Properties of Bamboo Activated Carbon Activate using Potassium Hydroxide Assisted by Microwave-Ultrasonic Irradiation," *ASEAN Journal of Chemical Engineering*, vol. 21, pp. 211–224, 2021. [CrossRef] [Google Scholar] [Publisher Link]

[78] Duy Anh Khuong, Hong Nam Nguyen, and Toshiki Tsubota, "CO_2 Activation of Bamboo Residue after Hydrothermal Treatment and Performance as an EDLC Electrode," *RSC Advances*, vol. 11, pp. 9682-9692, 2021. [CrossRef] [Google Scholar] [Publisher Link]

[79] Tao Zheng et al., "Synthesis and Evaluation of Bamboo-Based Activated Carbon as an Electrode Material for Electric Double Layer Capacitor," *International Journal of Electrochemical Science*, vol. 17, no. 11, 2022. [CrossRef] [Google Scholar] [Publisher Link]

[80] Ju-Hwan Kim et al., "Bamboo-Based Mesoporous Activated Carbon for High-Power-Density Electric Double-Layer Capacitors," *Nanomaterials*, vol. 11, no. 10, pp. 1-15, 2021. [CrossRef] [Google Scholar] [Publisher Link]

[81] Weiqian Tian et al., "Bio-Inspired Beehive-Like Hierarchical Nanoporous Carbon Derived from Bamboo-Based Industrial by-Product as a High-Performance Supercapacitor Electrode Material," *Journal of Materials Chemistry A*, vol. 3, no. 10, pp. 5656-5664, 2015. [CrossRef] [Google Scholar] [Publisher Link]

[82] Chan Kim et al., "Feasibility of Bamboo-Based Activated Carbons for an Electrochemical Supercapacitor Electrode," *Korean Journal of Chemical Engineering*, vol. 23, pp. 592–594, 2006. [CrossRef] [Google Scholar] [Publisher Link]

[83] Tianfu Huang et al., "Bamboo-Based Activated Carbon @ MnO_2 Nanocomposites for Flexible High-Performance Supercapacitor Electrode Materials," *International Journal of Electrochemical Science*, vol. 10, no. 8, pp. 6312–6323, 2015. [CrossRef] [Google Scholar] [Publisher Link]

[84] Syed Comail Abbas et al., "Bamboo-Derived Carbon Material Inherently Doped with SiC and Nitrogen for Flexible Supercapacitors," *Chemical Engineering Journal*, vol. 433, no. 3, 2022. [CrossRef] [Google Scholar] [Publisher Link]

[85] Xinhong Zhou et al., "A Renewable Bamboo Carbon/Polyaniline Composite for a High-Performance Supercapacitor Electrode Material," *Journal of Solid-State Electrochemistry*, vol. 16, pp. 877–882, 2012. [CrossRef] [Google Scholar] [Publisher Link]

[86] Camila Zequine et al., "High Performance and Flexible Supercapacitors Based on Carbonized Bamboo Fibers for Wide Temperature Applications," *Scientific Reports*, 2016. [CrossRef] [Google Scholar] [Publisher Link]

[87] Xiufang Chen et al., "A Novel Hierarchical Porous Nitrogen-Doped Carbon Derived from Bamboo Shoot for High Performance Supercapacitor," *Scientific Reports*, 2017. [CrossRef] [Google Scholar] [Publisher Link]

[88] N.A. Echeverry-Montoya et al., "Fabrication and Electrical Response of Flexible Supercapacitor Based on Activated Carbon from Bamboo," *Physica Status Solidi C: Current Topics in Solid State Physics*, vol. 14, no. 3-4, 2017. [CrossRef] [Google Scholar] [Publisher Link]

[89] Zenghua Xu et al., "Green Synthesis of Fe-Decorated Carbon Sphere/Nanosheet Derived from Bamboo for High-Performance Supercapacitor Application," *Energy Fuels*, vol. 35, pp. 827-838, 2021. [CrossRef] [Google Scholar] [Publisher Link]

[90] Hao Chen et al., "Functional Biomass Carbons with Hierarchical Porous Structure for Supercapacitor Electrode Materials," *Electrochimica Acta*, vol. 180, pp. 241-251, 2015. [CrossRef] [Google Scholar] [Publisher Link]

[91] Xiaona Pang et al., "Synthesis of Bamboo-Derived Porous Carbon: Exploring Structure Change, Pore Formation and Supercapacitor Application," *Journal of Porous Materials*, vol. 29, pp. 559–569, 2022. [CrossRef] [Google Scholar] [Publisher Link]

[92] Xi Yang et al., "Porous Nanoplatelets Wrapped Carbon Aerogels by Pyrolysis of Regenerated Bamboo Cellulose Aerogels as Supercapacitor Electrodes," *Carbohydrate Polymers*, vol. 180, pp. 385-392, 2018. [CrossRef] [Google Scholar] [Publisher Link]

[93] Rakhmawati Farma et al., "Synthesis of Highly Porous Activated Carbon Nanofibers Derived from Bamboo Waste Materials for Application in Supercapacitor," *Journal of Materials Science: Materials in Electronics*, vol. 32, pp. 7681–7691, 2021. [CrossRef] [Google Scholar] [Publisher Link]

[94] M. Jayachandran et al., "Activated Carbon Derived from Bamboo-Leaf with Effect of Various Aqueous Electrolytes as Electrode Material for Supercapacitor Applications," *Materials Letters*, vol. 301, 2021. [CrossRef] [Google Scholar] [Publisher Link]

[95] Guoxiong Zhang et al., "Activated Biomass Carbon Made from Bamboo as Electrode Material for Supercapacitors," *Materials Research Bulletin*, vol. 102, pp. 391-398, 2018. [CrossRef] [Google Scholar] [Publisher Link]

[96] K.M. Ajay, and M.N. Dinesh, "Performance Studies of Bamboo-Based Nano Activated Carbon Electrode Material for Supercapacitor Applications," *Materials Today Proceedings*, vol. 46, no. 10, pp. 4510-4514, 2021. [CrossRef] [Google Scholar] [Publisher Link]

[97] Linlin Ji et al., "N, S Co-Doped Biomass Derived Carbon with Sheet-Like Microstructures for Supercapacitors," *Electrochimica Acta*, vol. 331, 2020. [CrossRef] [Google Scholar] [Publisher Link]

[98] Huang Gege et al., "High-Performance Hierarchical N-Doped Porous Carbons From Hydrothermally Carbonized Bamboo Shoot Shells for Symmetric Supercapacitors," *Journal of the Taiwan Institute of Chemical Engineers*, vol. 96, pp. 672-680, 2019. [CrossRef] [Google Scholar] [Publisher Link]

[99] Qiushi Wang et al., "In-Situ Grown Manganese Silicate from Biomass-Derived Heteroatom-Doped Porous Carbon for Supercapacitors with High Performance," *Journal of Colloid and Interface Science*, vol. 534, pp. 142-155, 2019. [CrossRef] [Google Scholar] [Publisher Link]

[100] Sheng Li Zhang et al., "Study on the Capacitance Performance of Activated Carbon Material for Supercapacitor," *Advanced Materials Research*, vol. 239-242, pp. 797-800, 2011. [CrossRef] [Google Scholar] [Publisher Link]